MEASUREMENTS OF FIBER/MATRIX INTERFACIAL PROPERTIES OF A UD-C/C COMPOSITE UP TO 2273 K

Takuya Aoki*, Ken Goto**, Toshio Ogasawara* and Hiroshi Hatta*
*Advanced Composite Technology Center, Institute of Aerospace Technology, Japan Aerospace Exploration Agency, 6-13-1 Osawa, Mitaka, Tokyo 181-0015, Japan
** Space Structure and Materials division, Institute of Space and Astronautical Science, Japan Aerospace Exploration Agency, 3-1-1 Yoshinodai, Sagamiara, Kanagawa 229-8510, Japan
Keywords: *C/C composite, Fiber/matrix interfacial properties*

Abstract

The interfacial properties between the fiber and matrix of a unidirectionally reinforced carbon/carbon composite (UD-C/C) were evaluated for temperatures up to 2273 K in vacuum by using fiber bundle push-out and push-back tests. In these tests, the fiber bundle in a specimen was extruded and pushed back in the opposite direction using a pushrod and a supporting fixture made of graphite. In the push-out tests, shear fractures were observed to occur primarily along the fiber/matrix (F/M) interfaces and occasionally within the matrix carbon over the entire test-temperature range. The tests conducted at 298 K before and after the degassing of the absorbed gaseous species in the specimens revealed that the interfacial shear strength τ^i_{max} and initial sliding stress τ^i_s significantly increase after the degassing. As a result, the τ^i_{max} and τ^i_s values of the UD-C/C measured in vacuum exhibited their maximum values at 298 K and gradually decreased with an increase in the test temperature up to 2273 K.

1. Introduction

The tensile strength of carbon-fiber-reinforced carbon matrix composites (C/Cs) is generally much lower than the expected values from the fiber strength and rule of mixture. The utilization of the fiber strength in C/Cs is usually less than 50% [1–4]. To clarify the factors yielding a low tensile strength, our group had examined the relationship between the fracture strain ε_{ult} in tensile tests and the interfacial shear strength at the fiber/matrix (F/M) interface for various C/Cs at room temperature [1–3]. The general conclusion drawn is that when the bonding between the fiber and the matrix is strong, ε_{ult} yields a low value. Since the fracture strain of the carbon matrices in C/Cs is very low, this conclusion suggests that the matrix fracture first occurs under the tensile loading of the C/Cs and the matrix crack immediately penetrates into the adjacent fibers when the F/M bonding is strong. In this case, the final brittle fracture occurs at a low value of ε_{ult}. In contrast, in the weak F/M bonding case, the matrix crack is deflected by the debonding at the F/M interface, resulting in a high ε_{ult} value. This conclusion is further verified by introducing intentional microdamage at the F/M interface. Goto et al. have evaluated the residual tensile strength of a cross-ply laminated C/C after cyclic tensile loading [4]. They reported that ε_{ult} increased after the cyclic tensile loading due to an increase in the number of microcracks at the F/M interfaces, i.e., the degradation of the F/M interfaces. In the study by Kogo et al., the F/M bonding of a C/C was intentionally weakened via slight oxidation at low temperatures [5]. The bending tests after the oxidation at 773 K with 1% weightloss yielded 40% strength enhancement of the original strength. Micro-observations revealed that this enhancement was caused by the partial debonding at the F/M interfaces. These results indicate that the evaluation of the F/M interfacial properties is necessary for understanding the mechanical behavior of C/Cs.

It is well known that the tensile strength of C/Cs increases at elevated temperatures in inert atmospheres and in vacuum [1, 6–8]. The change in the F/M interfacial properties with temperature is considered as one of the influential factors for strength enhancement. For evaluating the F/M interfacial properties of C/Cs at room temperature, several test methods such as single-fiber and fiber bundle push-out tests [1–2, 9], fiber bundle pull-out tests [10, 11], and microbond pull-out tests [12] are available. These tests are used to determine the interfacial shear strength when complete debonding occurs and the sliding stress after debonding.

However, to the author's best knowledge, no test has been attempted at elevated temperatures and no clear experimental data pertaining to high-temperature F/M interfacial properties of C/Cs are available. As a result, the temperature dependence of the mechanical behavior of the C/Cs has not been discussed based on the F/M interfacial properties directly measured at elevated temperatures.

The objective of this study is to evaluate the interfacial properties between the fiber and matrix of a unidirectionally reinforced (UD-) C/C at the elevated temperatures. Specially arranged fiber bundle push-out and push-back tests were conducted at temperatures up to 2273 K in vacuum. The effects of the experimental parameters, such as the diameter of the pushrod and embedded length of the loaded bundle, were also examined at room temperature.

2. Experimental Procedure

2.1 Material

The UD-C/C examined was fabricated by the preformed yarn (PY) method [1–3, 9] and supplied by Across Co., Japan. The reinforcing fiber, fiber volume fraction and final heat treatment temperature (HTT) were TORAYCA-M40B (Toray Co., Japan), 50% and 2273 K, respectively. As shown in Figs.1(a) and (b), the matrix carbon exhibit a graphene-layered structure aligned parallel to the fiber surface. Partial debondings are frequently observed around the fibers after the processing of the composite. These as-processed debondings are attributed to the shrinkage of the matrix precursor due to carbonization and the tensile thermal stress induced during cooling from the HTT due to the mismatch in the coefficients of thermal expansion (CTE) between the fiber and the matrix [13].

2.2 Fiber Bundle Push-out and Push-back Tests

Two types of test facilities—I and II—were used depending on the test temperature *T*. The first facility I shown in Fig.2 was used for the fiber bundle push-out tests at room temperature in ambient air. In this experiment, a fiber bundle was pushed out from a thin platelet specimen using a tungsten-carbide pushrod with a flat end. The objective is to determine the effects of the pushrod diameter *D* and embedded length *L* of the loaded bundle, which is equal to the specimen thickness with regard to the interfacial properties.

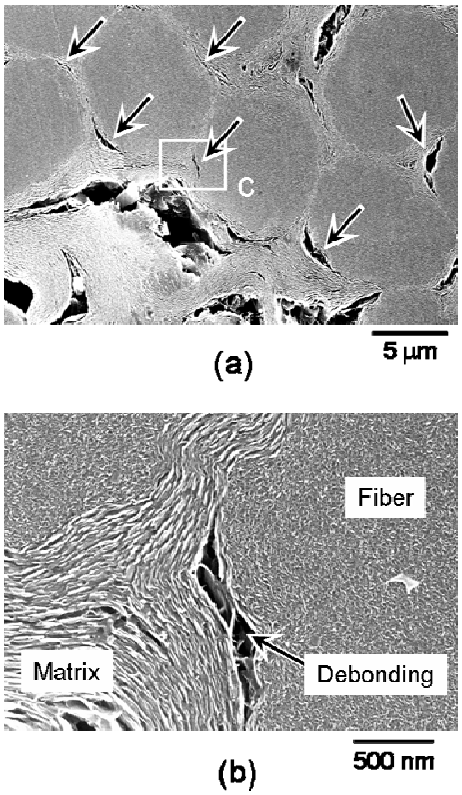

Fig.1 Cross-sections of the UD-C/C observed by SEM at different magnifications.

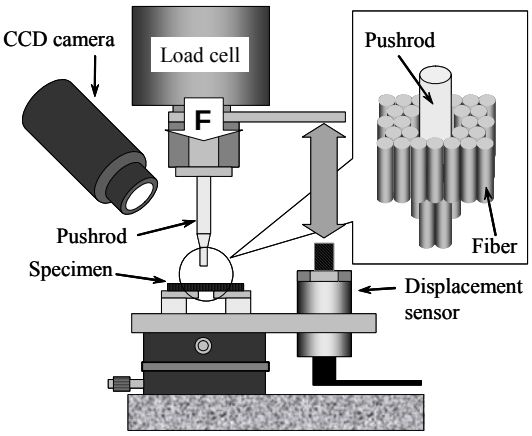

Fig.2 Schematic drawing of the fiber bundle push-out tests conducted at room temperature in ambient air (facility I).

The values of *D* and *L* were varied in the range from 50–300 μm and 100–300 μm. The thin specimens were prepared by mechanical polishing with diamond pastes [9]. These tests were conducted using a screw-driven testing machine (RTM-25,

Orientec Co. Ltd., Japan) at a displacement rate of 0.1 mm/min.

Figure 3 shows the test setup for facility II used for fiber bundle push-out and push-back tests at elevated temperatures. A specimen with a diameter of 11.5 mm and thickness of 4 mm was prepared such that the fibers were aligned along the thickness. A flat-bottom hole with a diameter of 3 mm was engraved on the specimen bottom up to a depth of ≈2.8 mm; the loaded bundle was then extruded into the hole. Thus, the embedded length L of the loaded bundle was ≈1.2 mm. A graphite cap was placed over the specimen and a graphite pushrod with $D = 2$ mm was set through the cap. The role of the cap is to prevent the pushrod from canting. The top surface of the specimens was polished to observe the fracture locations. In the push-back tests, the push-out-tested specimens were reversed and the extruded bundle was pushed back in the opposite direction.

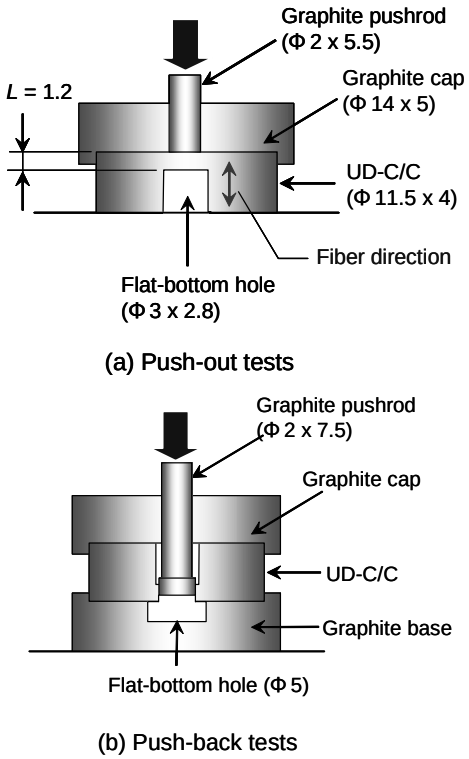

Fig.3 Schematic drawing of the fiber bundle push-out and push-back tests conducted at elevated temperatures (facility II).

The push-out and push-back tests were conducted at 298 K in ambient air and at temperatures up to 2273 K in vacuum (<1.5×10^{-2} Pa) at a displacement rate of 0.2 mm/min. To discuss only the effect of temperature on the interfacial properties, the room-temperature push-out and push-back tests were also conducted in vacuum after degassing the absorbed gases in the specimens. This degassing was performed by heating the specimens up to 1273 K in vacuum, followed by cooling to the room temperature. A screw-driven testing machine (8862, Instron, USA) equipped with a tungsten heater was used to apply the load. Prior to loading, the temperature of the specimens was maintained at the selected test temperature for 15 min. The temperature was measured using a tungsten/rhenium thermocouple set near the specimen up to 1873 K and using a two-color infrared thermometer for temperatures exceeding 1873 K.

3. Experimental Results

3.1 Effects of *L* and *D*

Figure 4 shows the typical load-displacement curve obtained from the push-out test at 298 K in ambient air. This result was obtained by using facility I with $D = 100$ μm and $L = 240$ μm. Initially, the applied load rapidly increased up to its maximum value F_{max}. A slight nonlinearity, wherein the load increased at a decreasing rate, was observed before F_{max} was attained. In this nonlinear region, debonding cracks are assumed to propagate incrementally from the defects such as voids and as-processed F/M debondings with the displacements. After F_{max}, the load abruptly drops to F_s and gradually decreases with a further increase in the displacements. As shown in Fig.4, the remaining bonded interface fractured catastrophically at F_{max}, and the loaded bundle began to slide.

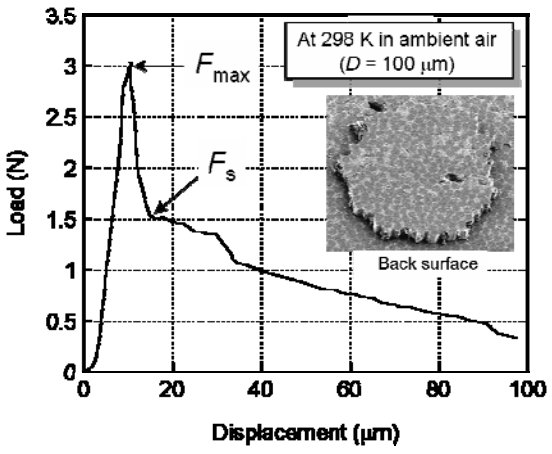

Fig.4 Typical load-displacement curve obtained by the push-out test at 298 K in ambient air.

Hence, F_{max} and F_s, respectively are regarded as the complete debonding load and the onset load of sliding.

Figure 5 shows F_{max} and F_s as functions of L when a pushrod with D = 50 μm was used. The F_{max} and F_s values linearly increase with the increase in L. This linear relationship indicates that F_{max} is not affected by the stress concentrations at the loaded bundle ends [14] and was observed independent of D within the examined range. Hence, the averaged interfacial shear strength τ^i_{max} over the interfacial area was used as a criterion for complete debonding and calculated as

$$\tau^i_{max} = \frac{F_{max}}{P_e L} \quad (1)$$

where P_e denotes the perimeter of the pushed-out bundle determined by scanning electron microscopy (SEM) after testing. The initial value of the sliding stress τ^i_s was calculated as

$$\tau^i_s = \frac{F_s}{P_e L} \quad (2)$$

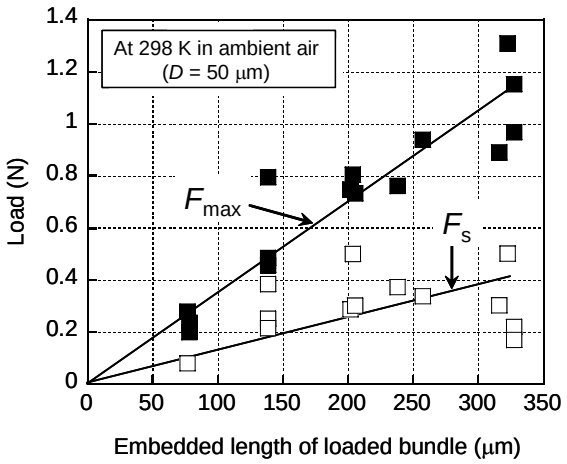

Fig.5 Debonding load F_{max} and sliding loads F_s obtained at 298 K in ambient air as a function of L of the loaded bundle.

Figure 6 shows the τ^i_{max} and τ^i_s values of the UD-C/C obtained at 298 K in ambient air as a function of D. In this figure, the results obtained by facility II with D = 2 mm are also plotted. The values of τ^i_{max} and τ^i_s rapidly decrease when D is increased from 50 μm to 300 μm and they exhibit nearly constant values in the D range from 300 μm to 2 mm. As shown in Fig.1, many voids and as-processed debonding cracks are observed in the F/M interfacial region. These defects are considered to act as a fracture source in the push-out tests. As D becomes larger, the probability of where these as-processed defects locate in the loaded region in the push-out tests becomes greater. Hence, the decreases in τ^i_{max} and τ^i_s with D are considered to be caused by the scale effect. This assumption is reasonable because the scatterings of τ^i_{max} and τ^i_s obviously decreased with increasing D.

The τ^i_{max} and τ^i_s values obtained in this study are regarded as representative values. The true strength at the bonded region of the F/M interface should be considerably greater than τ^i_{max} due to the presence of the as-processed defects. Although the apparent interfacial properties vary with D, we consider that the fiber bundle push-out tests are still effective to discuss the effects of the test temperature when a constant D is adopted in the series of tests.

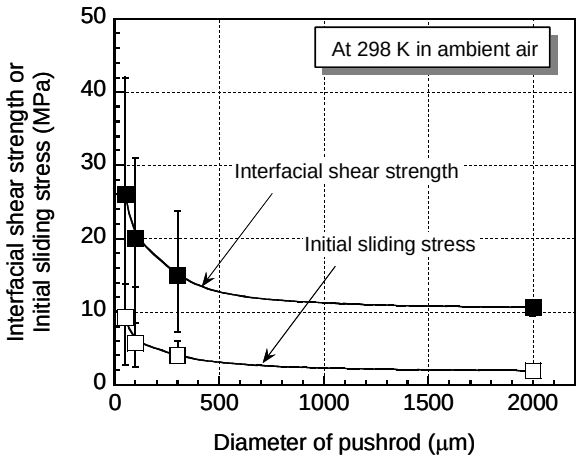

Fig.6 τ^i_{max} and τ^i_s obtained at 298 K in ambient air as a function of the pushrod diameter.

3.2 Push-out Test Results at Elevated Temperatures

The typical average interfacial shear stress–crosshead displacement (τ^i-δ) curves in the push-out tests at temperatures up to 2273 K are shown in Fig.7. Similar to the results obtained by facility I at room temperature, τ^i increased rapidly up to the maximum stress τ^i_{max}, followed by a large instantaneous drop for all the Ts. The typical fracture behavior is shown in Fig.8. The push-out experiments were successfully performed over the entire temperature range.

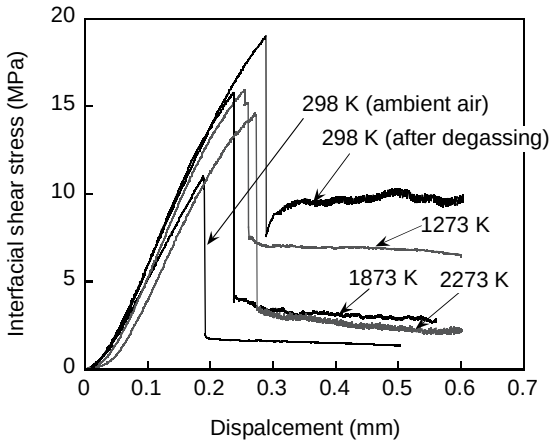

Fig.7 Typical τ^i-δ curves of the UD-C/C in the push-out tests from room temperature to elevated temperatures

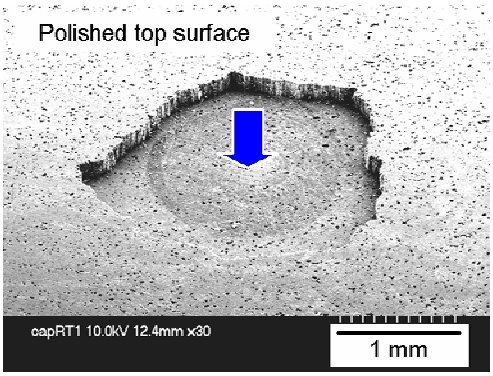

Fig.8 Typical top view of the push-out tested specimen.

Figure 9 shows the τ^i_{max} and τ^i_s values as a function of the *T*. At 298 K in ambient air, τ^i_{max} was approximately 11 MPa. The value of τ^i_{max} increased to ≈16 MPa at 1273 K and slightly decreased with a further increase in the temperature up to 2273 K, while τ^i_s at 298 K in ambient air was ≈2 MPa. The value of τ^i_s increased to ≈7 MPa at 1273 K, followed by a clear decrease at *T*s above 1273 K. It should be noted that at 298 K, τ^i_{max} and τ^i_s remarkably increased after the degassing of the absorbed gaseous species in the specimens. As a result, τ^i_{max} and τ^i_s have their maximum values at 298 K and gradually decrease with the *T* when only the effect of the *T* is considered.

The typical sliding surfaces on the pushed-out holes tested at 298 K in ambient air, at 1273 K and 2273 K are shown in Figs.10(a)–(c). A smooth surface with a small amount of debris is observed when τ^i_s is low, i.e., after the tests at 298 K in ambient air and at 2273 K. In contrast, a rough surface with a greater quantity of thin matrix debris is observed when τ^i_s is high (in the tests at 1273 K).

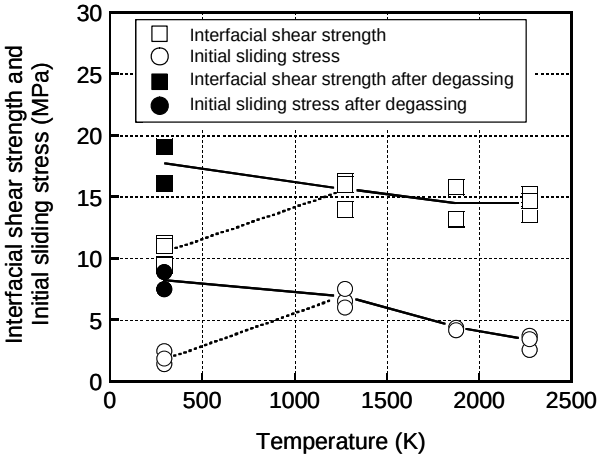

Fig.9 Temperature dependencies of τ^i_{max} and τ^i_s obtained for the UD-C/C by fiber bundle push-out tests.

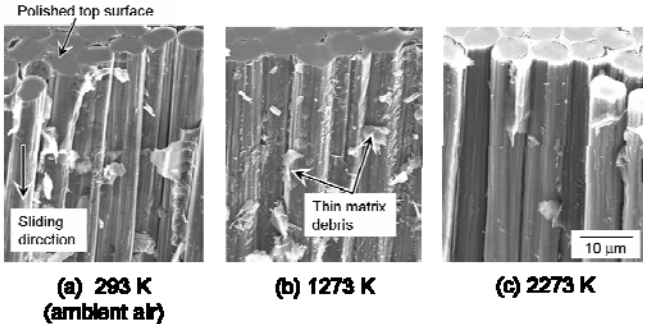

Fig.10 Sliding surfaces observed on the pushed-out holes tested at 298 K in ambient air (a) at 1273 K (b), and at 2273 K (c).

3.3 Push-back Test Results at Elevated Temperatures

In the push-back tests, the debonding of the loaded bundle has already been completed in the initial push-out tests. Thus, τ^i was calculated as

$$\tau^i = \frac{F}{P_e(L-\delta')} \quad (3)$$

where δ′ is the sliding displacement of the loaded bundle in the first push-out test. In this study, the first push-out test was completed when δ′ reached ≈0.3 mm; this was done to compare the push-back behaviors at different temperatures under identical conditions.

Figure 11 shows the typical τ^i-δ curves in the push-back tests at elevated temperatures. The maximum stress τ^i_{back} corresponds to the frictional stress required for the re-sliding of the extruded bundle in the opposite direction. Similar to the initial push-out test results, τ^i_{back} was low at 298 K in ambient air; it subsequently increased at 1273 K followed by a clear decrease in *T*s above 1273 K. A large enhancement in τ^i_{back} was also observed at 298 K after the degassing of the absorbed gaseous species. A comparison of the results between the push-out and push-back tests revealed that the magnitudes of the τ^i_{back} values were about 60% of those of the τ^i_s values in the initial push-out tests up to 1873 K. At 2273 K, the τ^i_{back}/τ^i_s ratio dropped to ≈0.3.

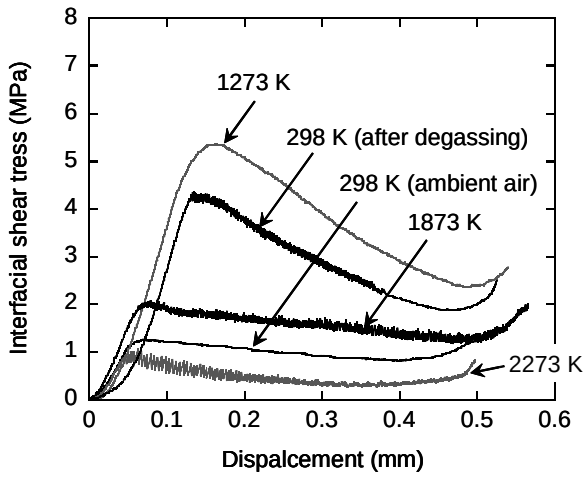

Fig.11 Typical τ^i-δ curves in the push-back tests of the UD-C/C at elevated temperatures.

4. Discussion

4.1 Fracture Location

Figures 12(a)–(c) show the typical fracture surface after the push-out tests stopped immediately after $\tau^i_{max.}$ The shear crack propagated preferentially along the F/M interfaces and occasionally within the matrix carbon. This conclusion regarding the crack path is verified in the secondary damage indicated by an arrow in Fig.12(a). Similar fracture behavior was observed over the entire *T* range. The matrix carbon of the UD-C/C has a graphene-layered structure, suggesting a low shear strength (Fig.1(c) and Fig.12(b)). However, the graphene layers are undulated due to the unevenness of the fiber surface and the presence of adjacent fibers. Hence, intensive interlocking by the graphene crystals is expected to occur against the crack propagation within the matrix (Fig.12(c)). As a result, the weakest path for the crack propagation in the push-out tests was considered to be that along the F/M interfaces. The presence of the as-processed F/M debonding further enhances the propagation at the F/M interfaces. These observation results demonstrate the effectiveness of the fiber bundle push-out tests for evaluating the F/M interfacial properties.

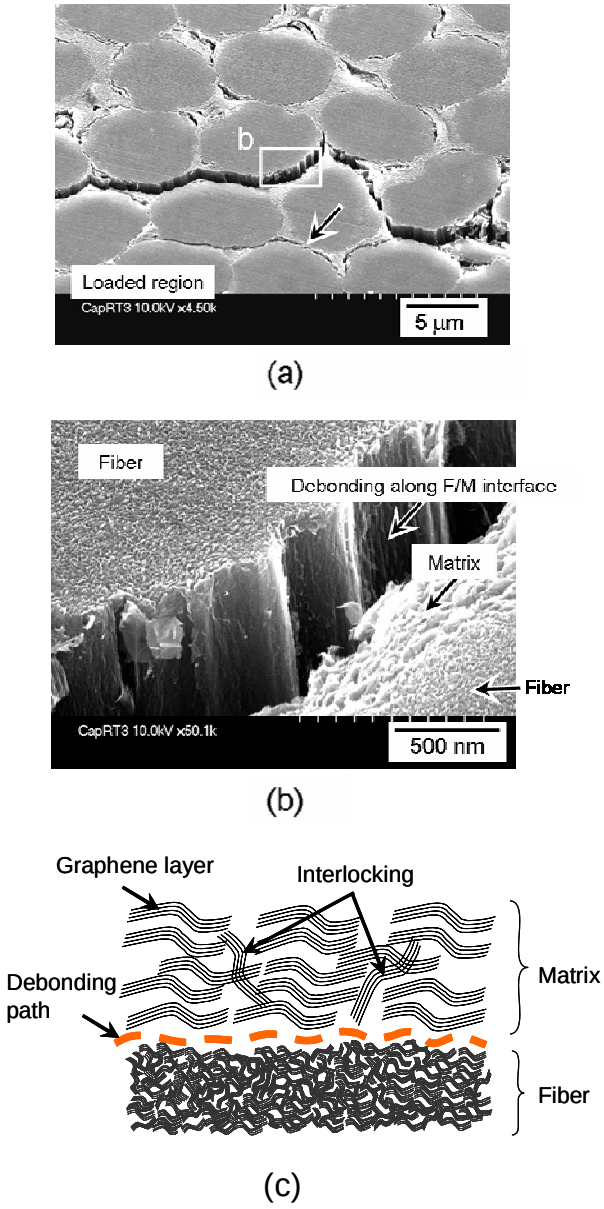

Fig.12 Typical fracture location observed after the push-out tests stopped immediately after F_{max}.

4.2 Effect of Degassing on Interfacial Properties

The values of τ^i_{max} and τ^i_s remarkably increased at 298 K after the degassing of the absorbed gaseous species in the specimens, as represented in Fig.9 by the closed squares and circles. Rowe reported that the friction coefficient μ and strength of polycrystalline graphite increase even at room temperature after the degassing of the absorbed water and oxygen [15]. In their tests, the value of μ for the degassed graphite was approximately 0.4 at room temperature, as compared to $\mu \approx 0.2$ before degassing. Rowe also reported that the graphite strength at room temperature increased by ≈40% after degassing. Similar enhancements in strength and μ due to degassing are reported for other graphites and various C/Cs [16–18]. Deacon et al. suggested that the edges of the graphene crystals react with water and oxygen in the atmosphere and form a surface containing various oxygenated groups. This surface layer reduces the adhesion between the graphene crystals and results in lower values of strength and μ [18]. In the push-out tests, the applied load is sustained by the elastic deformation of the bonded F/M interfaces and the friction at the surfaces of the as-processed F/M debonding cracks. Hence, the remarkable enhancements in τ^i_{max} and τ^i_s after degassing are considered to be caused by the removal of the oxygenated groups from the specimens.

4.3 Effect of *T* on Interfacial Properties

The influences of the *T* on the F/M interfacial properties are discussed in this section by referring to the test results of polycrystalline graphites at elevated temperatures. This is because the bonding at the F/M interface is achieved by the chemical reaction between the graphite crystals of the fiber and matrix. Further, the friction within the as-processed debonding cracks, which carries certain load in the push-out tests, occurs due to the contact between the graphite crystals.

The strength of carbon materials frequently increases with the *T*. For example, Sato et al. have reported that the compression strength of IG-110 graphite (Toyo Tanso Co., Ltd., Japan) increased by 40% at 2273 K as compared to that at room temperature. A similar extent of strength improvement has been reported at 2273 K for other polycrystalline graphites and graphite foam [7, 19]. Such strength enhancement of carbon materials suggests that the intrinsic bonding strength between the fiber and matrix of the UD-C/C may also increase at elevated temperatures.

There are additional mechanisms that can increase τ^i_{max} and τ^i_s at elevated temperatures. During cooling from the HTT to room temperature after the processing of the composite, a tensile thermal stress is induced at the F/M interface in the radial direction. This is because the radial CTE of the fibers is greater than that of the matrix carbon. Most of the stress can be released by the partial debonding of the F/M interfaces. However, thermal stress is considered to persist locally in the bonded F/M interfaces. This residual thermal stress should reduce τ^i_{max}. The CTE mismatch also affects the frictional resistance within the as-processed F/M debonding cracks. The opening of the debonding is expected to decrease with *T* due to the thermal expansion of each constituent. This closure increases the contact area in the debonding cracks. Hence, a greater load will be required for both the complete debonding and the sliding of the loaded bundle in the push-out tests at elevated temperatures.

On the contrary, however, the values of τ^i_{max} and τ^i_s measured in vacuum gradually decreased with the *T*, as shown in Fig.9. In particular, a clear decrease is evident for τ^i_s. This inconsistency suggests that adverse mechanisms that decrease τ^i_{max} and τ^i_s should act in tandem with the abovementioned increasing mechanisms. First, the tensile thermal stress induced during cooling from the HTT has been completely released due to the formation of the as-processed debonding and has a marginal influence on τ^i_{max} and τ^i_s enhancements. Second, the frictional resistance in the as-processed F/M debonding cracks decreased due to a decrease in μ at elevated temperatures. In fact, Rowe reported that μ of the graphite decreased from 0.4 to 0.1 when heated from 298 K to 2073 K in vacuum [15]. This decrease in μ may be caused by softening due to the high temperatures. As a result, the asperities and debris on the friction surface may be easily flattened. The enhanced stick-slip motion in which τ^i oscillates in the τ^i-δ curves with sliding at high temperatures (Fig.7 and Fig.11) may be attributed to the step-by-step flattening of the sliding surface. In conclusion, the decreases in τ^i_{max} and τ^i_s measured in vacuum with the *T* are assumed to occur as a result of the competition between the various increasing and decreasing mechanisms. Unfortunately, each contribution of the above influential mechanisms has not been quantitatively identified and is considered as a subject for future research.

A comparison between the results of the push-out and push-back tests provides information about the wear characteristics of the F/M interface. The ratio τ^i_{back}/τ^i_s was nearly constant at ≈0.6 from 298 K to 1873 K; however, it suddenly dropped to ≈0.3 at 2273 K. This decrease suggests that intensive wear has occurred during sliding. However, as shown in Fig.10(c), the sliding surface was very smooth with a small amount of matrix debris. These results indicate that the wear at 2273 K may occur at a microscale. The possible wear mechanism may be the flattening of the asperities at the debonded F/M interface due to the softening of the interfacial matrix. While τ^i in the push-back tests at 298 K after degassing and 1273 K remarkably decreased as the push-back test proceeded. This rapid decrease in τ^i also indicates that intensive wear has occurred. However, the mechanism seems to be different than that at 2273 K because the interfacial matrix should be rigid in such a low-temperature regime. Further, many thin matrix debris is observed as shown in Fig.10(b). Hence, the wear at 298 K after degassing and at 1273 K may be caused by the mechanical interlocking of the matrix debris at the debonded F/M interface.

5. Conclusions

The interfacial properties between the fiber and matrix of a UD-C/C were evaluated up to 2273 K by fiber bundle push-out and push-back tests. The conclusions obtained are as follows:

1. The shear fracture in the fiber bundle push-out tests of the UD-C/C occurred primarily along the F/M interfaces from room temperature to 2273 K. Hence, the fiber bundle push-out tests were considered to be effective for evaluating the F/M interfacial properties.
2. The interfacial properties of the UD-C/C measured by the fiber bundle push-out tests depended on the pushrod diameter due to the scale effect. Both τ^i_{max} and τ^i_s rapidly decreased when D was increased from 50 μm to 300 μm and exhibited nearly constant values in the D range from 300 μm to 2 mm.
3. The degassing of the absorbed gaseous species in the specimen remarkably increased τ^i_{max} and τ^i_s as compared to those before degassing. As a result, τ^i_{max} and τ^i_s measured in vacuum exhibited their maximum values at 298 K and gradually decreased with an increase in the T up to 2273 K.
4. The changes in τ^i_{max} and τ^i_s with T were assumed to occur as a result of the competition between several decreasing and increasing mechanisms.

References

[1] Hatta, H., Goto K., Aoki T., "Strengths of C/C composites under tensile, shear, and compressive loading: role of interfacial shear strength". *Compos. Sci. Tech.* , Vol. 65, pp2550–62, 2005.

[2] Hatta H., Aoi T., Kawahara I., Kogo Y., Shiota I., "Tensile strength of carbon/carbon composites I: Effect of density and interfacial strength". *J. Compos. Mater*., Vol.38, No.19, pp1819-26, 2004.

[3] Zaldivar R.J., Rellick G.S., Yang J.M., "Fiber strength utilization in carbon/carbon composites". *J. Mater. Res.*, Vol.8, No.3, pp501-11, 1993.

[4] Goto K., Hatta H., Katsu D., Machida T., "Tensile fatigue of a laminated carbon-carbon composite at room temperature". *Carbon*, Vol.41, pp1249-55, 2003.

[5] Kogo Y., Iijima Y., Igata N., "Enhancement of internal friction of carbon–carbon composites by selective oxidation". *Journal of Alloys and Compounds*, Vol.355, pp154-60, 2003.

[6] Goto K., Hatta H., Oe M., Koizumi K., "Tensile strength and deformation of a two-dimensional carbon-carbon composite at elevated temperatures". *J. Am. Ceram. Soc.*, Vol.86, No.12, pp2129-35, 2003.

[7] Sato S., Kurumada A., Iwaki H., Komatsu Y., "Tensile properties and fracture toughness of carbon-fiber felt reinforced carbon composites at high temperature". *Carbon*, Vol.27, No.6, pp791-801, 1989.

[8] Dzyuba V.S., Oksiyuk S. V., "Investigation of strength of carbon-carbon composite materials at temperatures from 293 to 3300 K under high-rate heating", *Strength of Materials*, Vol.37, No.1, pp99-104, 2005.

[9] Goto K., Kawahara I., Hatta H., Kogo Y., Shiota I., "Measurement of fiber/matrix interface properties of C/C composites by single fiber and fiber bundle push-out methods". *Composite Interfaces*, Vol.12, No.7, pp603-16, 2005.

[10] Valette L., Rouby D., Tallaron C., "Analysis of pull-out and failure of unidirectional bundles in a laminated carbon/carbon composite". *Compos. Sci. Tech.*, Vol.62, pp513-18, 2002.

[11] Sakai M., Matsuyama R., Miyajima T., "The pull-out and failure of a fiber bundle in a carbon fiber reinforced carbon matrix composite". *Carbon*, Vol.38, pp2123-31, 2000.

[12] Fujita K., Sakai H., Iwashita N., Sawada Y., "Influence of heat treatment temperature on interfacial shear strength of C/C". *Composites Part A*, Vol.30, No.4, pp497-501, 1999.

[13] Appleyard S.P., Rand B., "The effect of fiber-matrix interactions on structure and property changes during the fabrication of unidirectional carbon/carbon composites". *Carbon*, Vol.40, pp817-34, 2002.

[14] Kim J.K., Mai Y.W., "Engineered interfaces in fiber reinforced composites", Elsevier, 1998, pp93–169.
[15] Rowe G.W., "The friction and strength of clean graphite at high temperatures". *Wear*, Vol.3, No.6, pp454-62, 1960.
[16] Maruyama T., Nishimura Y., "Effect of adsorbed gases on mechanical properties of nuclear graphite". *Tanso*, Vol.152, pp98-105, 1992.
[17] Chen J.D., Lin J.H., Ju C.P., "Effect of humidity on the tribological behavior of carbon–carbon composites". *Wear*, Vol.193, pp38-47, 1996.
[18] Deacon R.F. and Goodman J.F., "Lubrication by lamella solids". *Proc. R. Soc. Lond.*, Vol.A243, pp464-81, 1958.
[19] Bruneton E., Tallaron C., Gras-Naulin N., Cosculluela A., "Evolution of the structure and mechanical behavior of a carbon foam at very high temperatures". *Carbon*, Vol.40, pp1919-27, 2002.